Characterization of Poly(ethylene oxide) Drawn by Solid-State Extrusion

Donald J. Mitchell† and Roger S. Porter*

Polymer Science and Engineering Department, Materials Research Laboratory, University of Massachusetts, Amherst, Massachusetts 01003. *Received October 1, 1984*

ABSTRACT: Samples of coextruded poly(ethylene oxide) (PEO), drawn to ratios of up to 31, were prepared and studied by using techniques of X-ray diffraction, birefringence, differential scanning calorimetry (DSC), and dynamic mechanical analysis (DMA). The amorphous component was found to orient first on draw, this occurring up to a draw ratio of 3–4. The crystalline component oriented as the draw ratio was increased from 3 to 12, as seen by the crystalline orientation function f_c which increased in that interval from 0.28 to 0.943. A value of 0.975 was obtained for f_c at a draw ratio of 28. Measurements of the crystallite size distributions from line broadening showed that the crystallite size in the direction of draw first decreased, reaching a minimum at draw ratios of 11–20, and then increased at higher ratios. The final average crystallite size in the draw direction was 291 Å compared to 271 Å for draw ratio 3.8. A significant result was the increase in crystallite size, after initially decreasing with draw, in the transverse direction at the highest draw. This indicates that for PEO draw by coextrusion produces growth in the width of the crystallites as well as length. For this case the increase is from 208 Å at draw ratio 20.5 to 247 Å at draw ratio 28. For both the draw direction and the transverse direction there is a much smaller increase in the growth of the crystallite size when annealed at a constant temperature. DSC thermograms of annealing after draw showed two peaks, one at a higher temperature and one at a lower temperature than the unannealed sample. This phenomenon persisted to higher draw ratios than previously reported, and its presence does not seem to be related to peak melting temperature, as previously suggested. Dynamic mechanical analysis showed the loss peak associated with the glass transition beginning at ever higher temperatures with increasing draw ratios and with a marked decrease in the slope of the tan δ vs. temperature curve. The results of this PEO study are consistent with a model for the formation of extended-chain molecules with draw and a resultant morphology where the mobility of the polymer chains is restrained because they either are part of or are closely associated with the extended-chain system.

Introduction

Solid-state extrusion of high molecular weight polymers has been shown to impart unusual properties.[1-5] Among properties that change in this drawing process are melting points, tensile modulus, birefringence, and crystallite orientations. To investigate further this process, samples of poly(ethylene oxide) (PEO) have been coextruded and the results reported here and in part 1[6] of this work. Poly(ethylene oxide) was chosen because of its simple linear structure and its crystalline nature. Moreover, prior PEO drawing studies are few compared to the exhaustive reports on PE deformation. PEO is also of interest because of its differences in chain packing compared to polyethylene (PE). Replacing every third methylene group in a PE chain with an oxygen increases the molecular weight of the repeat unit by ~5%; however, the density of the polymer is considerably higher (by some 23% in the crystalline state).

The samples have been studied by using X-ray analysis, dynamical mechanical analysis (DMA), and differential scanning calorimetry (DSC). The X-ray analysis consisted of determining the Herman–Stein orientation function at different draw ratio and the determination of crystallite size, also as a function of draw ratio, from line breadths for both annealed and unannealed samples. It was intended that the X-ray analysis would elucidate what happens to the crystalline portion of the polymer during the drawing process. By comparison of these results with measured birefringence which measures total orientation, insight could also be gained as to changes occurring in the amorphous regions. Dynamic mechanical testing was also used as a means to examine the changes taking place in the amorphous and crystalline regions. Differential scanning calorimetry was used as a method of examining the effect of annealing on the extrusion-drawn PEO.

Experimental Section

The PEO was obtained from Polyscience Corp. and was cited as having a molecular weight of 300 000. This PEO was used directly as received. Samples were prepared by melting the PEO in a hot press at 110 °C for 10 min followed by pressing at 15 000 psi for 5 min. Some samples were cooled slowly while under pressure, and others were cooled more quickly, both under pressure and at atmospheric pressure. These differences in cooling conditions had no noticeable influence on the drawing behavior nor on the subsequent PEO properties. Strips of PEO pressed film about 6 cm in length, 3 mm wide, and 2 mm thick were cut and used in the initial extrusion draw tests. Multiple coextrusions were used to obtain the higher draw ratios. The coextrusion process has been detailed elsewhere.[1] It should be noted that in drawing these relatively thick samples, the most effective draw was obtained by cutting the surrounding polyethylene billet longitudinally, but off axis, giving a thicker and a thinner section. A channel was machined along the length of the thicker section so that when the sample was inserted it was roughly coaxial with the assembled billet.

X-ray Analysis. Photographs of the diffraction pattern were recorded on flat film cassettes in a Statton type (Warhus) camera with Ni-filtered Cu radiation. Azimuthal scans for orientation function calculations and two θ scan profiles were obtained by using a Siemens Model D500 wide-angle automated diffractometer. All diffractometer work was done in transmission mode by using Ni-filtered Cu radiation. Beam divergence was minimized in line-broadening measurements by using incident and receiving beam slits of 0.10° and 0.018°, respectively. Under these conditions a standard simple of carefully dried hexamethylenetetramine had an integral breadth of 0.098° at 2θ = 17.84°.

The PEO peaks were recorded at every 0.05° and peak heights of between 600 and 900 counts s^{-1} for the 120 reflection and 13–25 counts s^{-1} for the much weaker 009 reflection were recorded. Background in the area of these peaks was 3–5 counts s^{-1} for the 120 reflection and 2–3 counts s^{-1} for the 009 reflection. Counting times of 15 s per point for the 012 reflection and 1 min per point for the 009 reflection were used.

† On sabbatical leave from the Department of Chemistry, Juniata College, Huntington, PA.

0024-9297/85/2218-1218$01.50/0

Table I
Crystallite Sizes (Angstroms) Determined from the 012 and 009 Reflections

	drawn unannealed		drawn annealed				
(a) EDR	(b) assuming Cauchy profile	(c) assuming Gaussian profile	(d) assuming Cauchy profile	(e) assuming Gaussian profile	av of Cauchy and Gaussian cases (f) unannealed	(g) annealed	(h) decrease in crystallite size with annealing
			012 Reflection				
3.8	328	250	540	366	282	453	171
6.7	254	204	403	294	229	348	119
11.1	229	187	311	240	208	278	70
20.5	230	187	274	216	208	245	37
23	257	205	285	224	231	254	23
28	276	218	298	232	247	265	18
			009 Reflection				
3.8	305	237	436	314	271	375	104
6.7	278	221	418	305	250	362	112
11.1	317	298	354	267	280	310	30
20.5	276	342	331	253	248	293	45
23	306	237	345	262	272	304	32
28	330	253	357	270	291	313	22

The Rachinger correction[7] was applied, but at these angles was no significant for line breadth. Integral line breadths were calculated by

$$\Delta\beta_{obsd} = (1/I_{max}) \int I(2\theta)\, d(2\theta)$$

where I_{max} is the maximum peak intensity. Since it was assumed that both crystallite size and distortions were contributing to the breadth of the peak profiles, instrument broadening effects were calculated by assuming both Cauchy and Gaussion profiles. The corrections are, for Cauchy $\Delta\beta_{cor} = \Delta\beta_{obsd} - \Delta\beta_{instr}$ and for Gaussian $\Delta\beta_{cor} = (\Delta\beta_{obsd}^2 - \Delta\beta_{inst}^2)^{1/2}$.

The mean crystallite sizes were calculated for both cases by using Scherrer's equation[8]

$$D_{hkl} = K\lambda/(\Delta\beta_{cor} \cos\theta_{hkl})$$

where K is taken as 1.0 and λ is the wavelength of the radiation used.

Crystallite orientation was determined by using the Herman–Stein orientation function[9,10]

$$f_{c,z} = \tfrac{1}{2}(3[\cos^2\phi_{c,z}] - 1)$$

where $\cos^2\phi_{c,z}$ is the mean square cosine, averaged over all the crystallites, of the angle between the c crystallographic axis and z, the draw direction. With the Wilchinsky method[11,12] $\cos^2\phi_{c,z}$ can be calculated from the relationship

$$\cos^2\phi_{c,z} = 1 + \{(2e_{110}^2 - 1)[\cos^2\phi_{120,z}] - (2e_{120}^2 - 1)[\cos^2\phi_{110,z}]\}/\{e_{120}^2 - e_{110}^2\}$$

where $\cos^2\phi_{120,z}$ and $\cos^2\phi_{110,z}$ are determined experimentally by the relationship

$$\cos^2\phi_{hkl,z} = \frac{\int_0^{\pi/2} I(\phi) \sin\phi \cos^2\phi\, d\phi}{\int_0^{\pi/2} I(\phi) \sin\phi\, d\phi}$$

and e_{110} and e_{120} are direction cosines between the plane normals of the 110 and 120 reflections, respectively, and a reference coordinate system. Details of the Wilchinsky method can also be found in an excellent treatment by Alexander.[13]

Mechanical Testing. The dynamic mechanical testing was performed on a Rheovibrón Model DDV-II at a frequency of 11 Hz. The heating rate was approximately 1 K min^{-1}. The tensile testing was carried out on a Instron universal testing machine using crosshead speeds of 0.10 cm min^{-1} and a 1 or 2 kg full scale range. Moduli were calculated at 0.1% elongation.

Differential Scanning Calorimetry. DSC scans were developed by using a Perkin-Elmer Model DSC-2 with thermal analysis data station. Temperature calibration was carried out by using benzophenone (mp 321.3 K) and 2 mg of naphthalene (mp 353.3 K). The melting points of the PEO samples were in the range 330–345 K. A scan rate of 5 K min^{-1} was used.

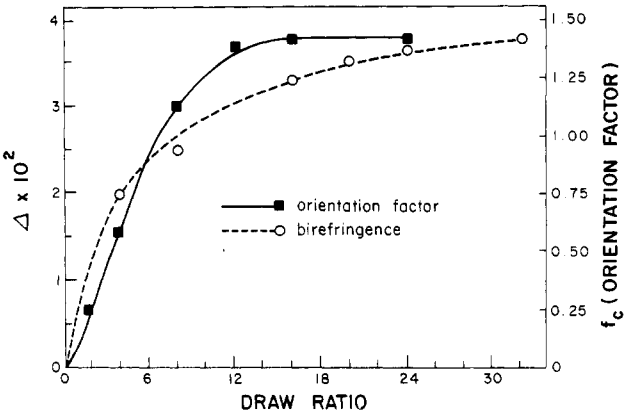

Figure 1. Chain orientation on uniaxial draw by birefringence, Δ, and crystal orientation, f_c.

Results and Discussion

X-ray. The diffraction pattern as recorded on a wide-angle photograph was similar to that reported by Takahashi and Tadokoro.[14] However, no traces of the planar zigzag modification reported by Takahashi, Sumita, and Tadokoro[15] were observed in either the photographs or the diffractometer scans.

The values of crystalline orientation function and birefringence as a function of draw are shown in Figure 1. The figure shows that birefringence rises more rapidly at lower draw ratios than does crystal orientation. Between draw ratios 4 and 10 the crystalline phase undergoes most of its orientation and by a draw ratio of 12 appears to have leveled off. The birefringence, in contrast, continues to increase, albeit more slowly even at the highest draw. The initial more rapid increase in the birefringence, which measures both crystalline and amorphous anisotropy, indicates that the first orientation is the amorphous intercrystalline regions. This is followed by orientation of the crystallites at intermediate draw. The noncrystalline portions continue to orient even at higher draw. Figure 2 depicts this process.

X-ray Crystallite Size. Table I gives values of the crystallite sizes as determined by line broadening for both the 012 and 009 reflections and for both annealed and unannealed samples. The line broadening of the 012 reflection gives an indication of the crystalline size in the transverse direction, while the 009 reflection gives and indication of crystallite size in the longitudinal, i.e., draw,

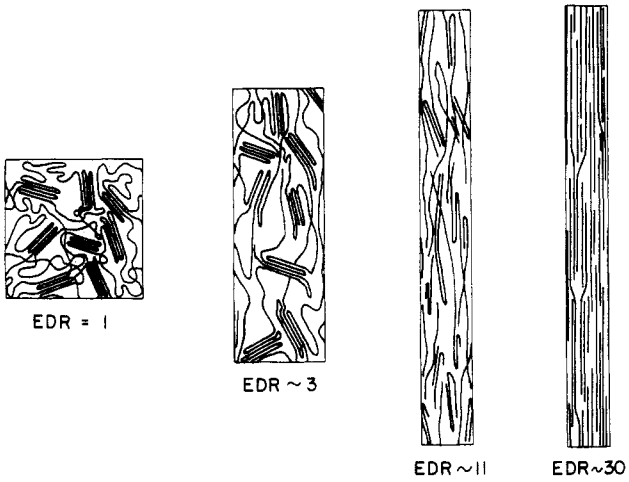

Figure 2. Chain models for crystalline and amorphous regions as a function of extrusion draw ratio, EDR.

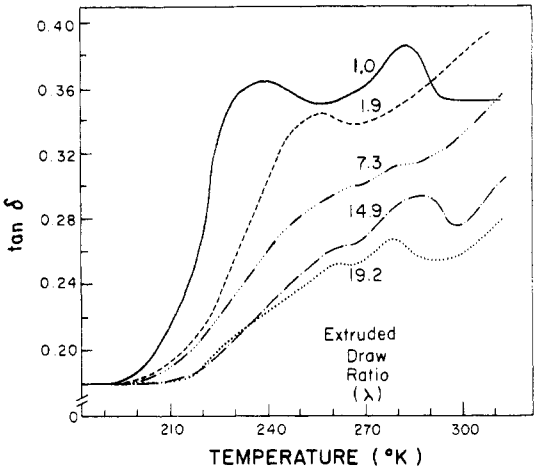

Figure 3. Tensile loss tangent, tan δ, as a function of temperature for a sequence of draw ratios.

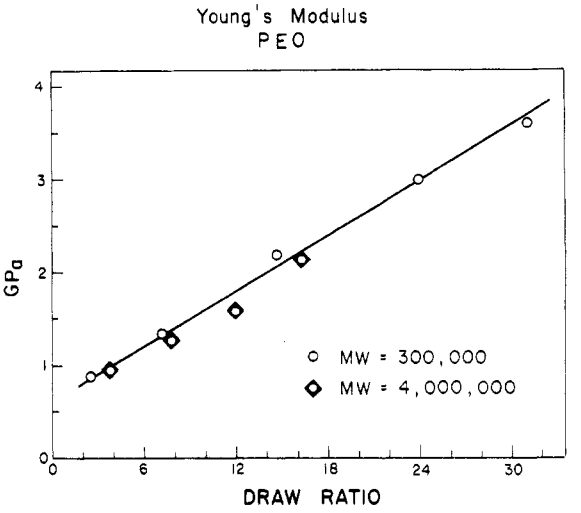

Figure 4. Tensile Young's modulus increase with extrusion draw ratio for PEO.

direction. Recall that paracrystallinity in addition to crystalline size contributes to line broadening. Thus, the values for crystallite size are considered to be a lower bound.

In columns f and g of Table I, we have listed the crystallite sizes obtained by averaging the values obtained by assuming Cauchy and Gaussian line profiles. Several trends are obvious. First, the sizes of the crystallites are seen to initially become smaller as the draw ratio is increased, reaching a minimum at a ratio of 11.1–20.5, then increasing only slightly with further draw. The only anomaly to this trend is the 009 reflection at a draw ratio of 11.1 in the unannealed state. Annealing of the drawn samples does not change this trend or anomaly. For both reflections and at all tested draw ratios, there is an increase in crystallite size with annealing (see column h, Table I). For the 012 reflection a steady decrease is observed in the effect of annealing at a constant temperature. The same general trend is seen for the 009 reflection except that the annealing effect is not as large at low draw and appears to approach a constant draw ratio of 11.

The general behavior exhibited by these crystallite size measurements is not inconsistent with observations of Kanomato and co-workers[5] for coextruded polyethylene. They observed the 200, 020, and 002 reflections show a decrease in crystallite size reaching a minimum at draw ratio of ~7. At higher draw they observed a marked increase in crystallite size from the 002 direction. As in the present case of PEO, at the highest draw they obtained a larger crystallite size in the direction of draw than initially present.

An interesting difference from Kanamoto's results is our observation for PEO of an increase in the crystallite size, as measured in the 012 direction at higher draw. This indicates that large chain extensions are being developed in the transverse direction. To our knowledge, this effect has not been previously reported. It may well be that this feature is produced here because coextrusion is a process carried out under compression.

Our findings on crystallite size as a function of draw are consistent with the chain-extended model of Peterlin.[16,17] The initial decrease in crystallite size with draw is viewed as a pulling out of chains and other disruptions of the original crystallites. As extended chains are formed in greater degree at higher draws, the average crystalline dimension in the draw direction increases. The decrease in the effect of annealing at higher draw is also reasonable in that as more of the polymer is found in extended chains, the amount of unconstrained polymer is reduced.

Dynamic Mechanical Analysis. Figure 3 shows the loss tangent, tan δ, as a function of temperature for PEO samples at several draw ratios, as measured on a Rheovibron. The undrawn sample shows two clear loss peaks, the first beginning at 203 K with a maximum at 230 K, and the second peak with a maximum at ~283 K. The temperature of the first peak is similar to that reported as the T_g of PEO. Enns and Simha[18] and Lang, Noel, and LeGraund[19] (the latter citing Boyer's upper and lower glass transition theory[20]) attribute this transition to amorphous chains restrained by crystallites. As the curves in Figure 3 show, as draw increases, the temperature at which T_g begins increases from ~203 to ~220 K. Also noticeable is the decrease in the height of the transition in its persistence to higher temperatures. This is consistent with a model of amorphous chains attached or under restraint by crystallites becoming increasingly ordered and restrained on draw. It is noted that this transition is not observed for single crystals of PEO,[21] further evidence that the origins of this peak lie in the amorphous regions of the polymer chain. It is likely that the second peak reported here also corresponds to a crystalline transition. Various authors[18,20,22] have reported transitions between −16 and +24 °C and invariably have assigned them to crystalline transitions.

The tensile moduli of the samples prepared in this study are shown as a function of draw in Figure 4. For comparison, consistent results obtained on a higher molecular

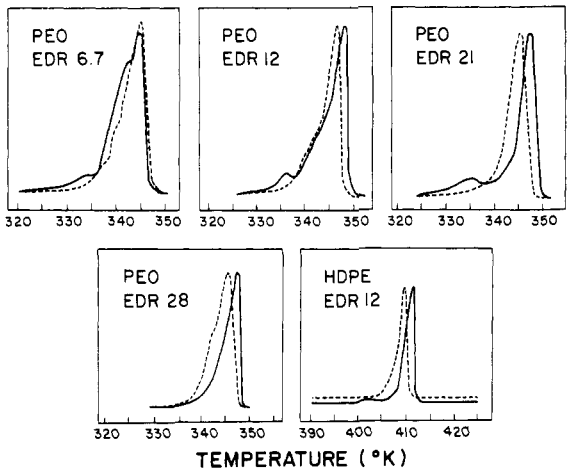

Figure 5. DSC data for PEO drawn to a series of extrusion draw ratios (dashed lines), followed by annealing at 332 K (solid lines). A comparison is made with a high-density polyethylene deformed to an extrusion draw ratio of 12.

weight PEO are also shown. The results with these thicker samples are similar with the thinner samples used in part 1 of this study.[6] A linear relationship is obtained for the tensile modulus as a function of draw.

Thermal Analysis. Figure 5 shows DSC data on PEO at several draw ratios and also after annealing at 332 K for 70 h, expressed as dashed and solid lines, respectively. We find reorganization qualitatively similar to reports on high modulus PE, i.e., the splitting of the thermogram into two peaks at a higher and lower temperature than the original peak.[5,23] The effect recorded for PEO differs in that it is persistent to a higher draw. Also, our annealing temperature is approximately 13 K below the peak melting temperature, which puts it at the extreme edge of endotherm recorded for the unannealed sample. The annealing temperature used for PE was approximately 5 K below the peak melting temperature and well within the melting peak envelope.

It has been postulated[23] that the important parameters for this effect are the breadth of the melting endotherm and the temperature difference $\Delta t = T_{Peak} - T_{Ann}$. However, for PEO we found the unannealed sample of draw ratio 21 to melt 0.5 K above the sample of draw ratio 28 and while the draw ratio 21 PEO showed the splitting effect and draw ratio 28 sample did not. We concur that the breadth of the melting endotherm is important, especially the breadth prior to the peak temperature. That is, as the melting peak narrows, this signifies more of the polymer either is incorporated into the extended-crystal region or is at least constrained by the extended-chain region. At the highest draw, this constraint is sufficient to prevent significant reorganization on annealing. Reorganization on annealing at a temperature on the very edge of the melting endotherm raises the possibility that the reorganization involves more than just melting and recrystallization.

Conclusions

The results on uniaxial draw of PEO are consistent with the formation of chain-extended crystals at higher draw. This conclusion is supported by the increase in crystallite size in the draw direction at high draw ratios, by the shift to higher temperature and smaller loss peak for the amorphous T_g transitions (recorded by dynamical mechanical analysis) by the increase in melting temperature for the drawn sample, and by the lack of formation of a double-peaked thermogram with annealing for the highest draw ratio.

The amorphous regions have been found to orient more quickly at draw ratios up to 4 with the crystalline regions completing the majority of their orientation by a draw ratio of 12. Results are consistent with a model of fibers that have been formed by the drawing out of lamellae at lower draw being brought into registry to form thicker crystals at the highest draw ratios. The formation of the double peak in the thermogram up to draw ratios of 21 on annealing at a temperature well below the peak melting temperature indicates that a critical parameter in the origin of this effect is the breadth of the thermogram for the unannealed state.

Acknowledgment. This work was supported in part by the Office of Naval Research.

References and Notes

(1) W. T. Mead and R. S. Porter, *J. Polym. Sci., Polym. Symp.*, **63**, 289 (1978).
(2) J. H. Southern and R. S. Porter, *J. Macromol. Sci., Phys.*, **4**, 541 (1970).
(3) T. Kanamoto, A. E. Zachariades, and R. S. Porter, *J. Polym. Sci., Polym. Phys. Ed.*, **17**, 2171 (1979).
(4) N. E. Weeks and R. S. Porter, *J. Polym. Sci., Polym. Phys. Ed.*, **12**, 635 (1974).
(5) A. Tsuruta, T. Kanamoto, K. Tanaka, and R. S. Porter, *Polym. Sci. Eng.*, **23**, 521 (1983).
(6) Part 1 for this paper: B. S. Kim and R. S. Porter, *Macromolecules*, preceding paper in this issue.
(7) W. A. Rachinger, *J. Sci. Instrum.*, **25**, 254 (1948).
(8) H. P Klug and L. E. Alexander, "X-Ray Diffraction Procedures", Wiley, New York, 1954, Chapter 9.
(9) P. H. Hermans and P. Platzek, *Kolloid-Z.*, **88**, 68 (1939).
(10) R. S. Stein, *J. Polym. Sci.*, **31**, 327 (1958).
(11) Z. W. Wilchinsky, "Advances in X-Ray Analysis", Vol. 6, Plenum Press, New York, 1963, p 231.
(12) Z. W. Wilchinsky, *J. Appl. Phys.*, **30**, 792 (1959).
(13) L. E. Alexander, "X-Ray Diffraction Methods in Polymer Science", Kriegen, Huntington, NY, 1979, p 245.
(14) Y. Takahashi and H. Tadokoro, *Macromolecules* **6**, 672 (1973).
(15) Y. Takahashi, I. Sunita, and H. Tadokoro, *J. Polym. Sci., Polym. Phys. Ed.*, 11, 2113 (1973).
(16) A. Peterlin, *Polym. Eng. Sci.*, **18**, 488 (1978).
(17) A. Peterlin, *J. Mater. Sci.*, **6**, 490 (1971).
(18) X. Emms and R. Simha, *J. Macromol. Sci., Phys.*, **B13**, 25 (1977).
(19) M. C. Lang, C. Noel, and A. P. LeGraund, *J. Polym. Sci., Polym. Phys. Ed.*, **15**, 1319 (1977).
(20) R. F. Boyer, *J. Polym. Sci., Part C*, **50**, 189 (1975).
(21) M. Takayonagi, *Kobunshi*, **14**, 314 (1965).
(22) T. M. Conner, B. E. Read, and C. Price, *Polymer* **8**, 414 (1967).
(23) G. Capaccio, J. Clements, P. J. Hine, and I. M. Ward, *J. Polym. Sci., Phys. Ed.*, **19**, 1435 (1981).